Response of a plastic pipe buried in expansive clay

Chaminda Pathma Kumara Gallage (PhD, MEng, BSc.Eng, MIEAust)

Lecturer, School of Urban Development, Queensland University of Technology, Brisbane, QLD 4001, Australia, chaminda.gallage@eng.monash.edu.au

Derek Chan (MEng, BEng)

Postgraduate student, Department of Civil Engineering, University of Monash , Clayton, VIC 3800, Australia, derek.chan@eng.monash.edu.au

Jayantha Kodikara (PhD, BSc.Eng, CPEng, FIEAust)

Associate Professor, Department of Civil Engineering, University of Monash, Clayton, VIC 3800, Australia, T. P: +61399054963, Fax: +61399044944

jayantha.kodikara@eng.monash.edu.au

Notations:

σ = longitudinal stress

M = bending moment calculated using applied load and assuming simply supported conditions

I = second moment of area of pipe cross section

D_o = external pipe diameter

ρ_b = bulk density of soil

H = the pipe depth (200 mm)

Abstract

Failure of buried pipes due to reactive (e.g., shrinking/swelling) soil movement is a common problem for water and gas pipe networks in Australia and the world. Soil movement is closely related to seasonal climatic change and particularly the moisture content of soil. Although some research has been carried out to understand the effect of freezing and thawing of soils and temperature effects in colder climates, there is very limited research has been undertaken to examine the possible failure mechanisms of pipe buried in reactive soils. This study reports the responses of a two metre long polyethylene pipe buried in reactive clay in a box under laboratory conditions. The soil and pipe movements were measured as the soil was wetted from the bottom of the box. It was observed that the pipe underwent substantial deformation as the soil swelled with the increase of moisture content. The results are explained with a simplified numerical analysis.

Introduction

As the pipe asset ages, buried pipe failures or breaks have become a major concern to most water and gas utilities. Failures of these pipes can produce negative social, environmental and economic impacts to the community. Water main bursts can lead to the loss of water, traffic delays, damage to surrounding infrastructure, soil erosion and storm water main contamination, whereas failures of gas pipe can lead to hazardous conditions, even involving violent explosions. The water losses due to pipe breaks vary in different parts of the world and the costs of maintenance of pipe networks can be considerable amounting to billions of dollars worldwide. For instance, the cost of maintaining and replacing existing urban water assets in Australia is estimated to be in excess of $AU 1 Billion dollars (WSAA, 2008). In

1998/99, the water pipe network in Australia was approximately 175,000 km and up to 30% of water (in some councils) is considered unaccounted for including water lost from pipe leaks and bursts. Similar issues are associated with the gas pipe networks. Therefore, there is a clear need for undertaking research into minimising the maintenance cost for the water and gas industry that will lead to an advanced system for pipe management and prediction of pipe failure.

The factors that lead to buried pipe failures have been identified as corrosion, internal pressure, traffic loading, thermal stress due to pipe temperature, and bending due to poor bedding and the forces produced by swelling/shrinking clay (Makar et al., 2001, Rajani et al., 1995) There is clear statistical evidence locally and in some parts of the world that pipe failure is significantly affected by seasonal moisture and temperature changes (Ibrahimi, 2005, Jarrett et al., 2001, Kassiff and Zeitlen, 1962, Rajani and Kleiner, 2001). The existing models for pipe failure consider only some of physical variables, and the influence of soil and climate are not properly taken into account. Under Australian climatic conditions, it has been established that water and gas pipe failure rates rise markedly during summer and to somewhat lesser extent during winter (Chan et al., 2007, Gould and Kodikara, 2008, Gould and Kodikara, 2009, Rajani et al., 1995). Furthermore, the pipe failure data indicates that these effects are much more pronounced after a wet and then prolonged dry periods (e.g., 2001/2002), highlighting the susceptibility of the existing pipe network to the local climatic changes.

Previous work on Australian data (Gould and Kodikara, 2009) indicates that there is a close correlation between increased pipe failure rates, climate and soil type. The understanding inferred from this work is that during periods of hot, dry weather reactive clay soils shrink

due to a reduction in moisture content with the loss of support for the pipes, and during the winter or wet periods, the soil swell exerting upward pressure to the pipes. A study (Kassiff and Zeitlen, 1962) inferred that high stresses produced by swelling soil can lead to pipe rupture. Similarly, in cold climates, increased pipe failures have been noted during winter due to decrease of pipe temperature (Rajani et al., 1995, Lochbaum, 1993, Needham and Hove, 1981). Freezing and thawing of soils has also been blamed for pipe failure in colder climates (Seligman, 2000). In general the soil movement is uneven and bending stresses are induced on the pipes, increasing the potential for failure.

Although some evidence of pipe failure in reactive soils is available, direct experimental results of pipe behaviour in reactive soils, either in the field or laboratory are very limited. The report (Kassiff and Zeitlen, 1962) on measurement of buried pipe stresses in the field was probably one of the earliest studies in this area. The field study was undertaken by burying two asbestos cement pipes in a site in Israel that contained highly expansive clay. The study has compared the difference in stresses due to moisture variation of backfill material, seasonal change and irrigation. A definite relationship between soil moisture variation and the axial loading has been found and the bending stresses induced by soil swelling can be a major cause of pipe failures. More recent field instrumentation has been undertaken in Canada (Hu and Vu, 2006) for a water main buried in expansive soils. A 4 m long, 150 mm diameter asbestos cement pipe section buried at 2.9 m below ground surface was removed and replaced by an instrumented PVC pipe section. Soil moisture content, temperature, and earth pressure were monitored by sensors installed at various depths below and above the pipe level. Strain gauges installed on the PVC pipe around its perimeter measured the pipe strain and extensometer attached to the pipe measured the pipe deflection. The analysis of the preliminary results of this study showed the development stress in the pipe due to soil

temperature changes and pipe deflection due to soil movement (shrink/swell). Apart from these studies, experimental works on pipe failures in reactive soils are not commonly undertaken. At Monash University there is an on-going project on this topic with field measurements of pipe behaviour, and this paper presents the laboratory experimental results of a model polyethylene pipe tested in an instrumented model box filled with reactive clay soil. Although polyethylene pipes are used relatively recently, in many cases they are installed by trenchless methods and, hence, no special bedding is provided surrounding the pipes. Hence, the behaviour of these pipes directly buried in reactive soils is relevant to field conditions. The paper presents results of pipe displacements measured using a specially developed device and soil moisture and suction measurements during soil wetting. Finally, a simplified numerical procedure is presented to estimate the soil movement on the basis of the measured soil and pipe properties.

Soil used in the experiment

An expansive soil collected from Merri Creek in Victoria, Australia was used for this study, and will be herein referred to as Merri Creek Clay. Interestingly, Merri Creek clay, which is black in colour, is commercially mined for construction of cricket pitches in Victoria. The physical properties of the soil obtained from laboratory test procedures, following Australian standards (Standard Australia, 1995a, 1995b, 1995c, 1995d, 2003) are presented in Table 1. The result of the compaction test conducted in accordance with Australia standard is shown in Fig. 1. The mineral composition of the test material was determined using the commercial package SIROQUANT for X – ray diffraction (XRD) (Srodon et al., 2001), the results are shown in Table 2. The significance presence of clay minerals, including smectite imparts high reactivity to the soil.

Swelling properties of soil

To obtain swelling curves of Merri Creek clay, a specimen was re-moulded to a diameter of 75 mm and a height of 20 mm using clay with an initial water content of 13%, which was equivalent to the initial water content of the soil used in the box. The specimen was then set on an Oedometer apparatus and a seating surcharge load of 1 kPa was applied. After inundating the specimen with water, the vertical displacement was continuously monitored until its rate of movement became approximately zero. Dividing this maximum vertical displacement by the specimen's initial height, the free-swelling strain was calculated. Upon reaching the maximum vertical displacement, the specimen was compressed by increasing the vertical stress in steps. In this paper, "the swelling pressure" was defined as the stress required bringing the specimen height to its initial height (Nelson et al., 2006). At each loading step, the load was sustained until the vertical displacement became a constant value. The vertical strain was then plotted against the corresponding vertical stress to obtain the so called "swelling curve". Four swelling curves obtained for samples with four different initial dry densities (e. g., 1.15, 1.25, 1.42, 1.46 g/cm^3) are shown in Fig. 2. It can be seen clearly that both the free-swelling and the swelling pressure increase with an increase in clay density. Fig. 3 shows the swelling curve used in the numerical analysis of the pipe deflection. In this figure, the swelling data of soil with dry density of 1.15 g/cm^3 as applicable to the soil in the experiment are fitted with a polynomial curve to describe the complete swelling curve.

Triaxial tests on soil

The triaxial test was undertaken to obtain the unsaturated shear strength of the soil above the pipe in the soil box. The pipe was buried at a depth of 200 mm below the surface and therefore the quick undrained triaxial test was performed with a confining stress of 1 kPa. A

soil specimen measuring 150 mm in height and 75 mm in diameter was remoulded to the same average density of the soil used in the experiment (ρ_d = 1.15 g/cm^3) and moisture content of 45 %, which is equivalent to 92 % saturation. The test was started by applying 1 kPa of cell pressure. Subsequently, the specimens were compressed at a loading rate of 0.2 mm/sec. The test was stopped after an axial strain of 10 % was achieved and the specimen was then removed from the cell. Fig. 4 shows the deviator stress against axial strain relationship obtained from triaxial test results and the data were fitted with a polynomial function. This result was used in the analysis section of this paper.

Mechanical properties of Polyethylene pipe used

The Young's Modulus and Poisson's ratio of the (medium density polyethylene) pipe used in the soil box was determined by testing a 1.5 m long pipe, as shown in Fig. 5. The pipe was attached with 11 strain gauges (nine gauges to measure longitudinal strain and two gauges to measure hoop strain) and was tested in a flexural bending test configuration, as shown. Ten strain gauges were attached symmetrically on the top and the bottom of the pipe at five different sections along the pipe. Assuming simply supported conditions, the central load was increased until the central deflection of 15 mm was achieved. The measured strain and the central load were recorded during the test.

Young's Modulus of Polyethylene pipe

Fig. 6 shows the measured longitudinal strains on the pipe at five sections during loading. Longitudinal stresses, σ on the pipe surface at strain measuring locations were calculated using Equation 1, assuming simple bending conditions.

$$\sigma = \frac{M}{I} * \frac{D_o}{2} \quad (1)$$

where M is the bending moment calculated using applied load and assuming simply supported conditions, I is the second moment of area of pipe cross section, and D_o is the external pipe diameter. Fig. 7 shows the plot of calculated stress and measured strain at the bottom of section 1. An approximate linear relationship of stress and strain is used to find the Young's modulus according to Hook's law. Similarly, Young's moduli were calculated at each strain measuring location and as a result, the average Young's modulus was calculated to be approximately 700 MPa, which is within the recommended range of the Young's Moduli reported (300~1300 MPa) for polyethylene pipes (Bilgin et al., 2007). Hence, a Young Modulus of 700 MPa was used in the numerical analysis described later in the paper.

Poisson's ratio of Polyethylene pipe

The ratio between the lateral (hoop) strain and the longitudinal strain can be used to calculate the Poisson's ratio. As shown in Fig. 8, the measured hoop and longitudinal strains at the bottom of sections 2 and 4 are plotted and the Poisson's ratio of the pipe is given by the gradient of these graphs. The average value of the calculated Poisson's ratio is approximately 0.473 and it is within the range of the Poisson's ratios (0.42 ~ 0.50 (Bilgin et al., 2007)) reported for polyethylene pipes.

Model box test

The soil box used for the experiment was modified from a plastic water storage tank. As shown in Fig. 9, the soil box measured 1015 mm in depth, 720 mm in width and 1880 mm in length. In order to fit a pipe into the box, 112 mm diameter holes were drilled on the side

walls at both lateral and longitudinal directions, to allow for two possible pipe arrangements. In this experiment, the pipe was installed on the longitudinal direction, therefore the holes on other walls were sealed up by the plastic cover with bolts and rubber sleeves to stop possible water leakage. A transparent perspex sheet (Fig. 9) was also installed on one side of the box to observe the water level and soil movement during the experiment. The modified box was restrained by a steel frame with thick timber sheets fixed within the frame to provide adequate lateral restraints to the plastic box. It was aimed to minimise the soil swelling in the horizontal direction, making the soil movement to be mainly in the vertical direction, representing one-dimensional swelling conditions. Lateral deflection of the box has not been measured but the closely spaced steel frame along with thick timber sheet backing would be sufficiently stiff to restraint fully any horizontal swelling of the soil. Visual observations indicated that timber backing did not experience in visual deformations, in contrast to tens of millimetres of vertical movement experienced by the wetting soil, and therefore, the horizontal strains experienced by the soil over its length and width may be considered to be nearly zero.

Model box preparation

A 2180 mm long polyethylene pipe measuring the inner and outer diameters of 85 mm and 110 mm, respectively, was instrumented with 56 uniaxial strain gauges. Seven sets of strain gauges were installed at every 300mm along the pipe. Each set consisted of eight strain gauges measuring strain at four locations on the pipe circumference: top, bottom, left springline, and right springline. There were two gauges at each location: one gauge was oriented along the longitudinal axis of the pipe to measure the longitudinal strain and the other gauge was oriented perpendicular to the first gauge to measure the circumferential strain. After installing the strain gauges on the pipe and attaching wires with them, a waterproofing material (SEMKIT®) was applied on the strain gauges and surrounding area to protect the

gauges against moisture. It was then allowed approximately 24 hours for the waterproofing material to be cured, before the pipe was installed longitudinally in the box as shown in Fig. 10. The pipe ends were kept open and was accessible from both ends.

A 170 mm thick layer of gravel was placed on the base of the box in order to provide a permeable base. A layer of geotextile was then placed on the gravel as a separator between the soil and the gravel. The box was filled with Merri Creek clay, which had an initial water content of 13 % by using a wet-compaction method. The amount of wet soil required for pre-determined volume (layer) to achieve a dry density of 1.15 g/cm^3 was measured and placed in the box. After spreading the soil uniformly over the plan area of the box, the compaction was done in order to bring the soil surface to the pre-determined level. This procedure was followed until the box was filled completely. Three core samples have been then obtained by pushing a tube into the compacted clay, and on this basis, gave an average dry density of 1.15 g/cm^3 down the depth of the soil profile. During the filling of the box, strainpots, thermal conductivity sensors, theta probes and thermocouples were installed at designated depths to measure respectively the pipe and soil deformation, soil suction, volumetric soil water content, and soil temperature, as shown in Fig. 10. The surface of clay was covered up with wetted newspaper and plastic sheets after soil filling and compaction. The experiment was started by suppling water to the bottom of the box approximately 30 days after soil placement.

Experimental results and discussion

After setting up of the soil box as shown in Fig. 10, the wetting of the clay was started by supplying water from a Mariotte bottle so that zero water pressure was maintained at the bottom of the clay layer. In reality, wetting of soil is likely to occur from the top due to

rainfall and irrigation, except when there is a leak in the pipe. However in this instance, wetting from the bottom was adapted due to several reasons, main ones being to reduce the overall time for the testing and to facilitate better interpretation of results. It was considered to take much longer for water to infiltrate from the top through compacted clay, all the way to the bottom. And with any water pressure applied at the top to accelerate the water flow, as has been done with capillary rise method, water may bypass through (possible gaps in) sidewalls which could cause the interpretations very difficult.

As the experiment proceeded, the water level in the Marriotte bottle was raised to accelerate the soil wetting, as shown in Fig. 11 (change of zero water pressure level). The wetting process was continued for 136 days, and the responses of the installed sensors were recorded continuously. In the following section, the responses of sensors are presented and discussed.

Soil suction and water content

Three Campbell thermal conductivity sensors (TCS) calibrated to measure soil suction in kPa were used to measure soil suction in this experiment. The responses of these Campbell thermal conductivity sensors (TCS), installed in the soil box (see Fig. 10), are shown in Fig. 12. Suction sensors at different levels showed a similar response when the soil moisture content increased as the experiment proceeded. TCS-1, which is located 75 mm above the bottom of the clay layer, responded almost immediately when water was supplied to the box, as the suction decreased to zero corresponding to almost full saturation state and subsequently remained constant. The soil above the water level could be saturated due to capillary rise of water and therefore, TCS sensors could indicate the decrease in soil suction before the water external level was raised up to the sensor. Once the wetting water front reached a TCS sensor, the reading of the sensor drastically decreased to a value which is corresponding to saturated

soil. About 1 day after TCS-1 has responded to the change of moisture content, TCS-2 which was located 125 mm above the TCS-1 started to respond to the approaching wetting front. TCS-3 which was close to the surface stayed constant at the initial suction (100 kPa) for the first 36 days then showed a decrease in suction, about 10 days after raising the zero pressure level in the Marriotte bottle by 280 mm from its initial level. Eventually, TCS-3 reached zero suction (full saturation) about 66 days after starting the wetting of the soil box. These response times are consistent with capillary rise in low permeable materials as reported by (Lee et al., 2004), who indicated that water rose to 75 mm height less than a half day and 200mm in about 2 to 3 days and the rate of rise decreased dramatically with time as water rose higher.

Six moisture probes (MC) calibrated for Merri Creek clay to measure volumetric moisture content were installed in the soil box to measure the moisture content change during the test. However, only two probes (see Fig. 10) functioned well while the other four probes failed to function properly. As shown in Fig. 13, the moisture probe at 75 mm from the bottom of the clay layer (MC-1) measured an increase in moisture content immediately after the experiment had started and was reasonably constant throughout the experiment. This probe was close to the base of the soil where the moisture content was maintained by the water supply. MC-2 at 610 mm from the bottom of the clay layer responded in a delayed fashion but in harmony with water level increase. When comparing the responses of the suction probes and the moisture probes shown in Figs. 12 and 13, respectively, the suction and water content at the same level appear to change simultaneously without a time lag between them. The responses of both the suction and water content probes indicate the upward advancement of the wetting front with time.

Soil temperature

The locations of four temperature sensors (TP) buried at different depths within the soil box are shown in Fig. 10. Fig. 14 clearly highlights that the fluctuation of soil temperature at the various depths during the experiment was similar suggesting that change of temperature was largely due to surrounding temperature changes and was not significantly affected by the increase in soil moisture content.

As shown in Fig. 14, a significant drop of temperature can be identified from 64th day to 136th day after the experiment had started. During this period, the temperature decreased from a maximum of 23 °C to a minimum of 18.5 °C. On the basis of the measured ambient temperature generally, this temperature drop appears to coincide with the ambient temperature change.

Soil and pipe displacement

Soil displacements were measured from the movements of steel rods using strain pots (SP). Locations of some of the strain pots installed in the soil box are shown in Fig. 10. The soil displacement measurement was started when water was supplied at the bottom of the soil box. As shown by the solid lines in Fig. 15, with the start of soil wetting from the bottom, SP-1 and SP-2 located respectively at 230 mm and 330 mm above the soil bottom, progressively recorded upward movement indicating the swelling of soil with the increase in water content. SP-3 and SP-4, which were located on the top of the pipe, initially showed a slight (less than a one mm) downward movement. The reason for this small downward movement is not exactly clear, but could be due to soil settlement or possible shrinking of soil due to drying prior to wetting. It should be noted, however, that the soil was protected from drying by placing wetted newspaper and plastic on the top surface, prior to starting of the wetting experiment. With the rise of the water table, SP-3 and SP-4 started to show upward movement which

would be generated by the upward deflection of the pipe due to swelling of the soil below the pipe. As shown in Fig. 15, it is clear that the soil moves upward (swells) with an increase in water content. The pipe embedded in this swelling soil deflected upward with the soil movement as the swelling pressure built up under the pipe. Fig. 15 indicates that the degree of swelling depends on the confining pressure. In other words, as the confining pressure increases, the swelling displacement decreases. Though, water content and suction changed simultaneously as the wetting proceeded (Figs. 12 and 13), the soil swelling started with a certain time lag possible due to higher confining pressure at the bottom of the box.

Forty days after the experiment had started, the movements of the strainpot rods attached with measuring tapes graduated in mm were monitored by using a surveying level. This was undertaken as a back-up measurement. Fig. 15 shows that these level measurements (shown by symbols) and indicates that these measurements agree reasonably well with the strain pot measurements. However, human error in using survey level and the possible deformation of the measuring tapes attached with the strainpots could lead to the differences in these two measurements.

Since the strain gauges failed to respond accurately, the pipe deflection was measured along the pipe inserting a specially designed device into the pipe and using a surveying level, after 136 days of the commencement of wetting. The device used to measure the deflection on the pipe is shown in Fig. 16. This consisted of a ruler which is graduated in mm, which was fixed on a shuttle attached to a 2.5 m long steel rod and the ruler is pressed upward by a spring to maintain contact with the top of the pipe inside. The rod was pushed along the bottom of the pipe while the ruler in contact with the top of the pipe. A land surveying level was set up so that the line of sight was set through the pipe was used to read the ruler at every 100 mm

along the pipe. The measured deflection was plotted with the deflection of the pipe obtained from SP-3 and SP-4 and is shown in Fig. 17. As shown in this figure, the pipe deflection measured by the strain pots (SP-3 and SP-4) located directly on top of the pipe agreed well with the internal deflection of the pipe. The deflection of pipe measured this way is used for the numerical analysis described in the next section. This special device used to measure the pipe deflection was designed after realizing that the strain gauges had malfunctioned, hence, was used at the end of the test, but not at different stages of the wetting process.

Numerical procedure to predict the deflection of buried pipes

The distribution of measured internal pipe deflection (see Fig. 17) shows significant upward bending of a pipe buried in reactive soil. It may be at the mid pipe section, soil above the pipe may have experienced an average strain of about 6% (for 12 mm deflection over 200 mm soil), which may have led to shear failure of the soil at some locations (see Fig. 5). The pipe uplift prediction model for shallow buried pipes (Cheuk et al., 2005) shows that for a buried pipe to be deflected upward the uplift force of the pipe has to be greater than the uplift resistance force acting above the pipe. The ultimate uplift resistance can be considered to be the combination of the overburden load and the in situ shear stress along the inclined plane extending outwards from the pipe at the angle of soil dilation as shown in Fig. 18. This mode of deformation was verified by centrifuge testing on model pipe systems (Cheuk et al., 2005). Although they did not consider reactive soils in their study, the developed modes of failure can be considered to be applicable. In this study, the angle of dilation is assumed to be zero as applicable for undrained clay.

Fig. 19 shows the upward deflected pipe in equilibrium under the uplift and uplift resistance forces. The uplift force is caused by swelling of the soil under the pipe. The maximum swelling pressure is applied at the supports where the pipe upward deflection is restrained (zero swelling strain) and the minimum swelling pressure is applied at the mid pipe section where the maximum soil swelling occurs. As the upward pipe deflection increases, the soil strain above the pipe increases and subsequently the shear resistance of the soil above increases.

Swelling pressure acting on the pipe

The uplift force of the buried pipe is caused by the soil swelling pressure acting on the bottom of the pipe. The swelling pressure profile can be obtained by considering the measured deflection inside the pipe as presented in Fig. 17. Since the upward deflection of the pipe was due to swelling of the soil, the magnitudes of the soil displacements beneath the pipe were the same as the pipe deflection. The average swelling strain profile along the pipe is assumed to arise uniformly from the 430 mm thick soil layer below the pipe, although actual soil strains would vary with the soil depth. Therefore, the swelling strain profile can approximately be obtained by dividing the measured deflected profile from the thickness of the soil below the pipe (430 mm). The swelling pressure profile acting on the pipe can be obtained from the oedometer test results of the soil specimen with a dry density of 1.15 g/cm^3 in Fig. 3. The swelling pressure can be converted to a unit load along the pipe by multiplying by the pipe's outer diameter (110 mm). Fig. 20 shows the strain profile and swelling load profile acting on the pipe (uplift force) used for this simplified numerical analysis.

Soil resistance above the pipe

The average soil strain profile above the pipe is approximated by dividing the measured deflection of the pipe by the soil thickness above the pipe (200 mm). The resisting shear stress

profile can be obtained from the triaxial test result shown in Fig. 4. The soil shear stress corresponding to the pipe deflection was calculated as half of the deviator stress at corresponding strain level. The shear force considered in the analysis is calculated according to the model (Cheuk et al., 2005), where the shear force is considered to be acting along the shear planes extending outwards from the pipe at the angle of dilation. Since the angle of dilation is zero for undrained clay, the shear plane is considered to be extended vertically from the pipe to the soil surface. Therefore, the soil resistance (kN/m) on top of the pipe may be calculated using Equation 2.

$$\text{Soil resistance} = \text{Shear stress} \times 2 \times \text{soil depth to the pipe} \quad (2)$$

where the soil resistance is equal to the shear stress acting at the two shear planes along the depth of the pipe.

Surcharge load due to soil above the pipe

Apart from the swelling and resistance force, the overburden load of soil is also acting on the pipe. The analysis considered the soil moisture content at 45 % with dry density of 1.15 g/cm^3. The uniformly distributed surcharge load, P (kN/m) is then calculated using Equation 3,

$$P = \rho_b \times H \times D_o \quad (3)$$

where ρ_b is the bulk density of soil, H is the depth of the pipe and D_o is the pipe external diameter.

Results of analysis

All the calculated soil loads were applied to the pipe with the measured Young's modulus of 700 MPa, Poisson's ratio of 0.48, and moment of area of the pipe of 7.402 × 10^{-5} m^4 for

computer structural analysis. The pipe was analysed for bending using PROKON structural analysis software (Prokon Software Consultant, 2003) assuming two end support conditions, *i.e.*, pinned and fixed.

A comparison of the experimental and analysed pipe deflections shown in Fig. 21 indicates that the distribution of pipe deflection predicted using the simplified theoretical analysis is reasonably close to the measured deflection values. It is worth noting that maximum deflection occurred at the mid span in the theoretical results, where the measured maximum deflection is slightly shifted to the right side of the pipe possibly due to differential swelling of the soil. The numerical analysis results also confirm that the experimental buried pipe support is better represented by a pinned end support condition, as expected from the physical condition that was provided in the pipe box test set up.

The analytical results show that the upward pipe deflection occurred when the soil swelling stress increased while the soil resistance on top of the pipe reduced due to increase of the moisture content. Despite the significant approximations made, the pipe deflection predicted by the simplified theoretical analysis provides reasonable agreement with the measured values and therefore the theoretical procedure may be used to predict the approximate behaviour of pipe in the field when the required properties of pipe and soil are available. In the field analysis, it may be possible to apply an iterative numerical procedure, where the computation is preceded until the predicted and assumed deflections are matched. For example, when more deflection than actual is assumed, the pipe will deflect less because of the reduction of soil swelling pressures. So this procedure can be repeated until convergence is obtained in the predicted and assumed soil pressures following the non-linear swelling process. This analytical procedure is schematically shown in Figure 22. Some preliminary analyses

undertaken on field scenarios involving cast iron and plastic pipes with spans of 6 m indicate that pipe middle displacements of several millimetres for the cast iron and tens of millimetres for the plastic pipes may be possible. It should be noted that more accurate analysis of the pipe behaviour in this experiment will require resorting to a more standard numerical technique such as the finite element method. This would require a more detailed parametric input, characterising the unsaturated soil behaviour under large deformations.

It should be noted that for relatively rigid pipes like cast iron pipes, the upward deflection will be much smaller although the swelling pressure acting on the pipe will be higher. Furthermore, cast iron is much more brittle than plastic pipes and can experience failure at relatively low strain levels. The wetting events in the field are most likely from rainfall events on the top instead of capillary rise from the bottom, the rate of soil swelling may provide different stress profile for the pipe. Having said this, a major difference of soil/pipe interaction behaviour in wetting from top and bottom is the way wetting progresses with time. In order for pipe to get stressed due to wetting, the soil below the pipe should get wet. Hence, final result will be pretty much the same, when the soil below the pipe gets wetted by both methods. However, it is possible that the transient stages will be somewhat different due to the differences in the moisture regime down the soil profile.

Conclusions

This paper demonstrates the behaviour of a Polyethylene pipe buried in clay soil box subjected to wetting from the base. A simplified numerical procedure was developed to predict the deflection of a buried pipe in reactive soil using pipe and soil properties. Soil and pipe properties were obtained in the laboratory and the proposed iterative numerical

procedure was employed to predict the deflection of the buried Polyethylene pipe. The following conclusions can be drawn from the results of this study.

(1) It is clear that the water content and suction changed simultaneously as wetting proceeded, but the swelling movement is dependant on the overburden pressure, confinement and also displayed a certain time lag. Therefore it is necessary to take these into account in detailed and more rigorous modelling of the pipe/reactive soil interaction using standard continuum analysis methods.

(2) Both free swelling displacement and swelling stress increase with the increase in soil density.

(3) The simplified numerical analysis of pipe deflection capturing some of the essential mechanics has generated comparable results with the soil box experiment. This numerical procedure has provided information on the pipe bending mechanisms, which proved that the pipe movement was directly related to the properties of the pipe material and soil.

(4) When comparing with the field situation, the large scale soil box experiment did not consider the internal pressure of the pipe and the greater buried depth of the pipe in the field. These factors can provides higher resistance on the pipe and possibly reduce the upward deflection. But relatively rigid pipes like cast iron pipes, the upward deflection will be much smaller although the swelling pressure acting on the pipe will be higher. The soil box experiment has provided a useful simulation of a buried pipe bending due to change of soil moisture content in a laboratory situation, while the simplified

theoretical analysis was found to provide reasonable results comparable with the measured values, and may be applied to simulate the field conditions approximately.

Acknowledgements

This research was funded by a linkage grant from Australian Research Council in partnership with City West Water, Alinta, Envestra, SPAusnet, South East Water, Perth Water Corporation and Ipswich Water. Their cash and in-kind support to this project is gratefully acknowledged. The basic pipe box was provided by CSIRO. Thanks are also rendered to other researchers who provided some valuable input.

References

Bilgin, O., Stewart, H. E. & O'Rourke, T. D. (2007). Thermal and mechanical properties of polyethylene pipes. *Journal of Materials in Civil Engineering* **19**, No. 12, 1043-1052.

Cha,n D., Kodikara, J. K., Ranjith, P. G., & Choi, X. (2007). Data analysis and laboratory investigation of the behaviour of pipes buried in reactive clay. *10th Australia-New Zealand Conference on Geomechanics*, Brisbane, pp.206 – 211.

Cheuk C. Y., White D. J. and Bolton M. D. (2005). Deformation mechanisms during uplift of buried pipes in sand. *Proceedings of the 16th International Conference on Soil Mechanics and Geotechnical Engineering*, Osaka, pp. 2837-2840.

Gould S. and Kodikara J. K. (2008). *Exploratory Statistical Analysis of Water Reticulation Main Failures (Melbourne, Australia)*. Department of Civil Engineering, Monash University, Australia, Report RR11.

Gould S. and Kodikara J. K. (2009). *Exploratory Statistical Analysis of Gas Reticulation*

Main Failures (Melbourne, Australia). Department of Civil Engineering, Monash University, Australia, Report RR12.

Hu Y. and Vu H. Q. (2006). Field performance of water mains buried in expansive soil. 1st International Structural Specialty Conference, Calgary, Alberta, May 23-26.

Ibrahimi F. (2005). Seasonal variations in water main breaks due to climate variability and ground movement. *Proceedings of Australian Water Association (Ozwate),* Brisbane, pp. 28-35.

Jarrett R., Hussain O., Veevers A. and Van Der Touw J. (2001). A review of asset management models available for water pipeline networks. *Proceedings of International Conference on Maintenance Societies (ICOMS),* Melbourne, pp. 49-57.

Kassiff G. and Zeitlen J. G. (1962). Behaviour of pipes buried in expansive clay. *Journal of the Soil Mechanics and Foundations Division,* **88**, 132-148.

Lee K. Y., Kodikara J. K. and Bouazza A. (2004). Modelling and laboratory assessment of capillary rise in stabilised pavement materials, Transportation Research Record, 1868, pp. 3-1.

Lochbaum B. S. (1993). PSE&G develop models to predict main breaks. *Pipeline and Gas Journal*, **220**, 20-27.

Makar J. M., Desnoyers R. and McDonald S. E. (2001). Failure modes and mechanisms in gray cast iron pipe. *Proceedings of the Conference on Underground Infrastructure Research*, Ontario, pp. 1-10.

Needham D. and Hove M. (1981). Why gas mains fail: Part 1. *Pipe Line Industry*, **55**, 47-50.

Nelson J. D., Reichler D. K. and Cumberers J. M. (2006). Parameters for heave prediction

by oedometer tests. *Proceedings of the 4th International Conference on Unsaturated Soils*, Arizona, pp. 951-961.

Prokon Software Consultant. (2003). *Prokon (computer program for structural analysis)*, Ver. 1.8.

Rajani B. B. and Kleiner Y. (2001). Comprehensive review of structural deterioration of water mains: physically based models. *Urban Water*, **3,** No. 3, 151-164.

Rajani B., Zhan C. and Kuraoka S. (1995). Pipe-soil interaction analysis of jointed water mains. *Canadian Geotechnical Journal*, **33**, No. 3, 393-404.

Seligman B. J. (2000). Long-term variability of pipeline permafrost interaction in north-west Siberia. *Permafrost and Periglacial Processes*, 2000, **11**, 5-22.

Srodon J., Drits V. A., McCarty D. K., Hsieh J. C. C. and Eberl D. D. (2001). Quantitative X-ray diffraction analysis of clay-bearing rocks from random preparation. *Clays and Clay Minerals*, **49,** No. 6, 514-528.

Standards Australia. (1995a). *Determination of the liquid limit of a soil – Four point Casagrande method.* Standards Australia, Sydney, AS1289.3.1.1.

Standards Australia (1995b). *Determination of the plastic limit of a soil.* Standards Australia, Sydney, AS1289.3.2.1.

Standards Australia. (1995c) *Determination of linear shrinkage of a soil.* Standards Australia, Sydney, AS1289.3.4.1.

Standards Australia. (1995d) *Determination of the particle size distribution of a soil - Standard method of analysis by sieving.* Standards Australia, Sydney, AS1289.3.6.1.

Standard Australia. (2003). *Soil reactivity tests—Determination of the shrinkage index of a soil - Shrink-swell index.* Standards Australia, Sydney, 2003, AS1289.7.1.1.

WSAA. (2008). *The Australian Urban Water Industry*. Water Services Association of Australia, Report card 2007/2008.

Table 1: Properties of Merri Creek caly

Liquid limit, w_l [%]	73.30
Plastic limit, w_p [%]	33.00
Plasticity index, I_p [%]	40.30
Linear shrinkage [%]	13.30
Specific gravity, G_s	2.62
% passing sieve No. 200 (425 µm)	100.00
Clay content [<0.002 mm: %]	0.90
Silt content [%]	99.10
Maximum dry density $\rho_{d(max)}$ [g/cm^3]	1.36
Optimum water content [%]	26.40
Swelling stress [kPa] for ρ_d=1.15 g/cm^3	98.10

Table 2: Mineralogy content of Merri Creek clay

Quartz	Albite	Orthoclase	Kaolin	Smectite	Calcite	Halite	Ilmenite	Anatase
41	2	3	3	51	-	-	1	<1

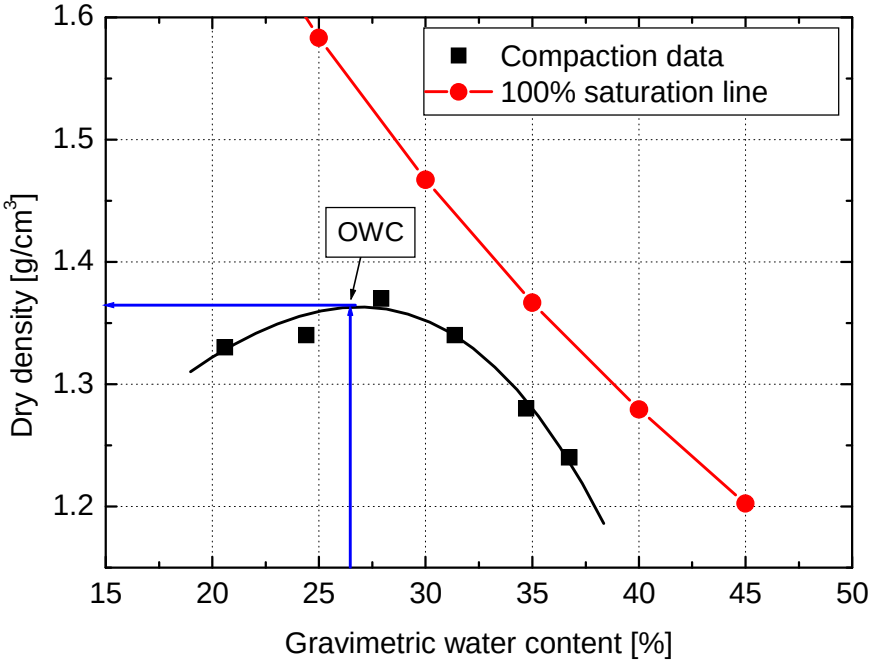

Figure 1: Standard proctor compaction curve for Merri Creek clay

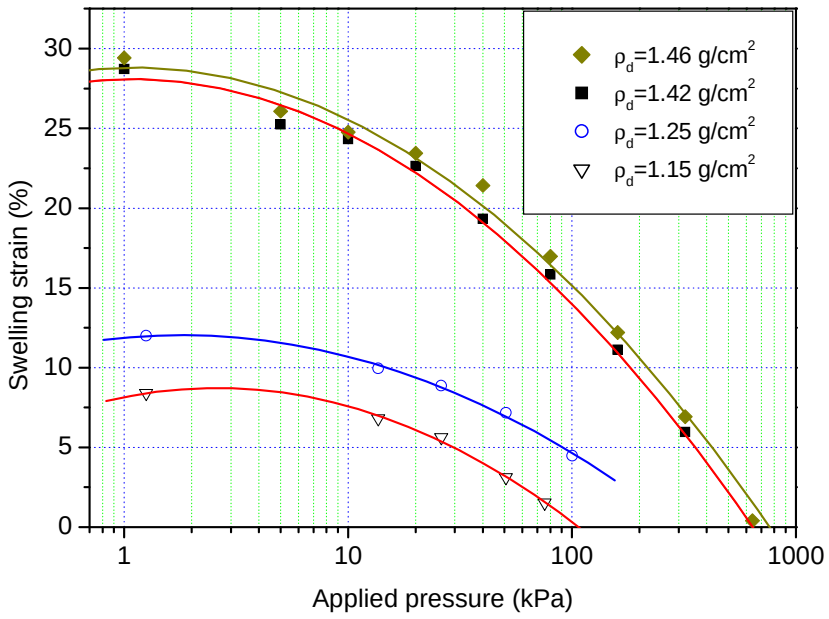

Figure 2: Variation of swelling pressure curves with initial dry density of soil samples

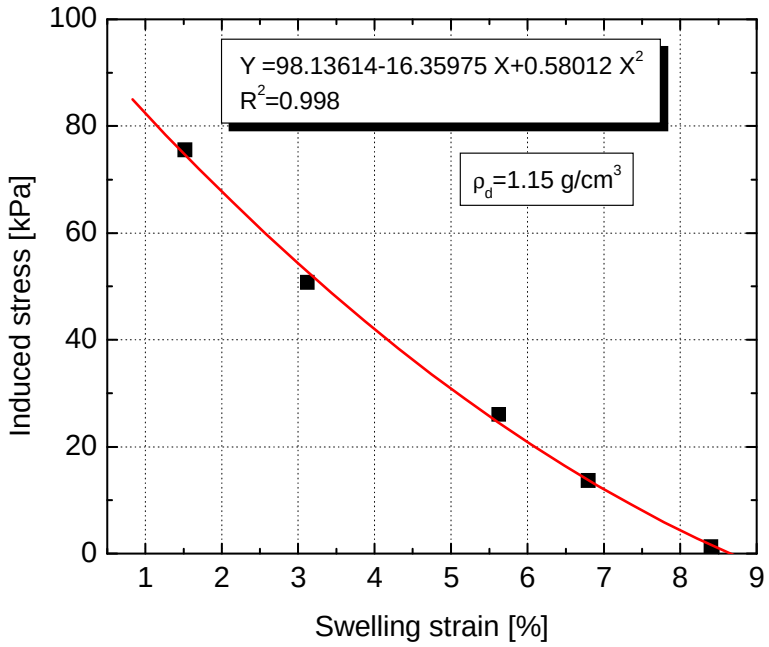

Figure 3: Swelling curve used for the numerical analysis of the pipe

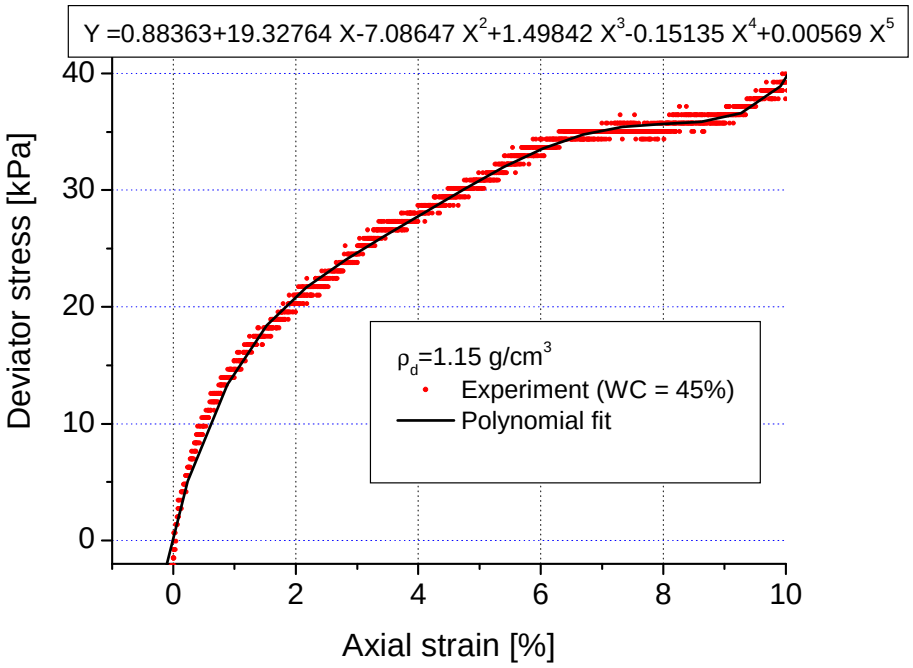

Figure 4: The triaxial test result used in the numerical analysis of the pipe

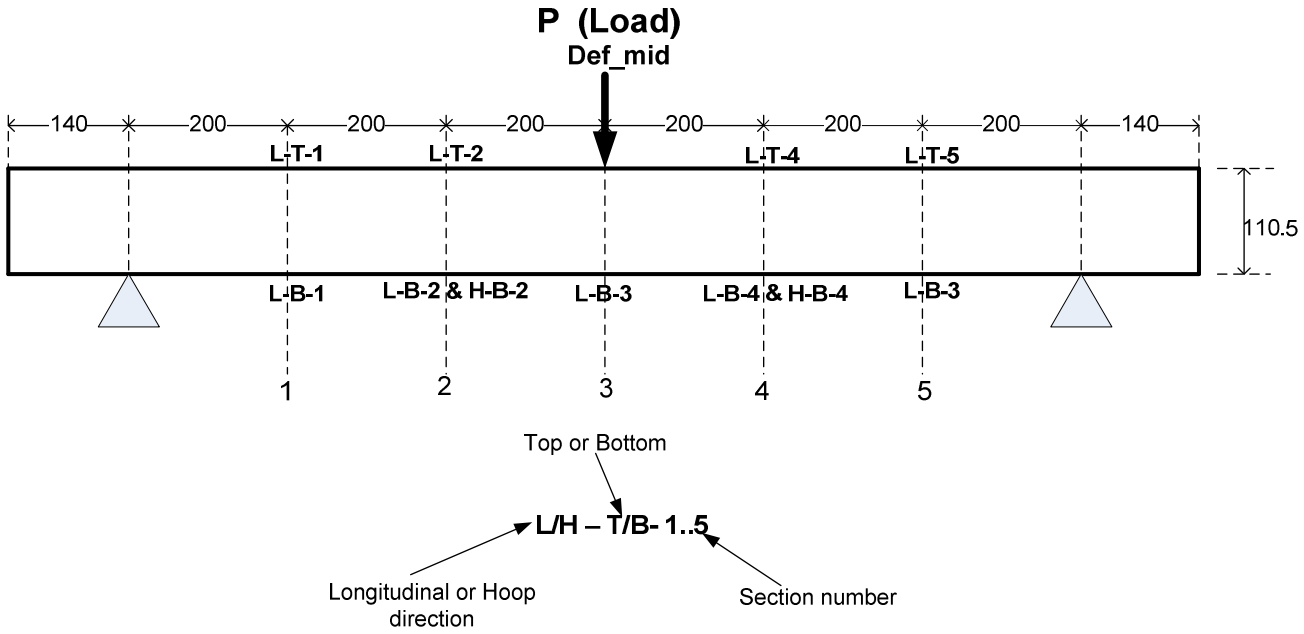

Figure 5: Strain gauge locations on the Polyethylene pipe used for three-point loading test

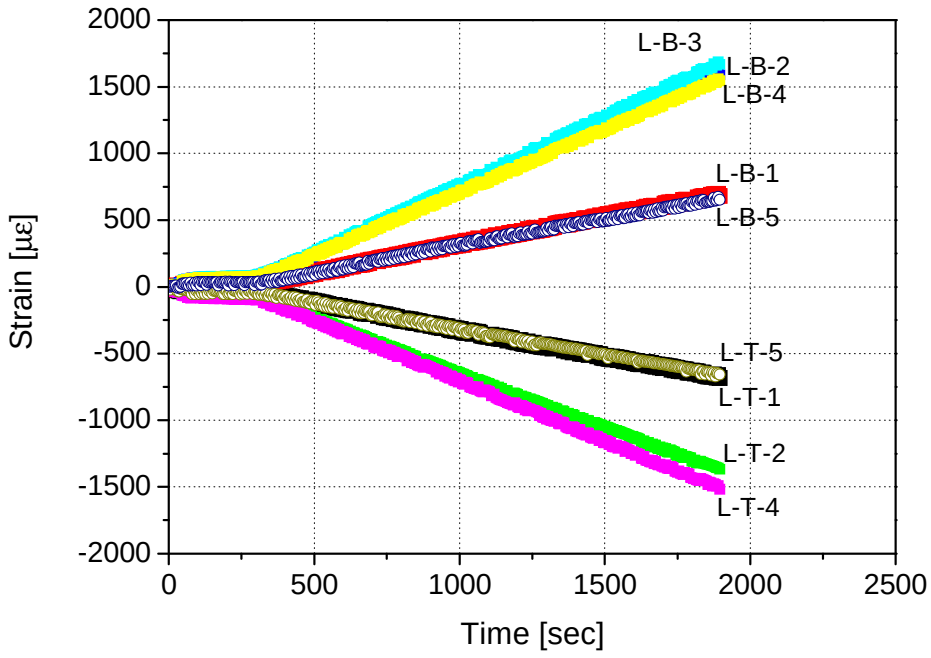

Figure 6: Time histories of responses of strain gauges used in three-point loading tests

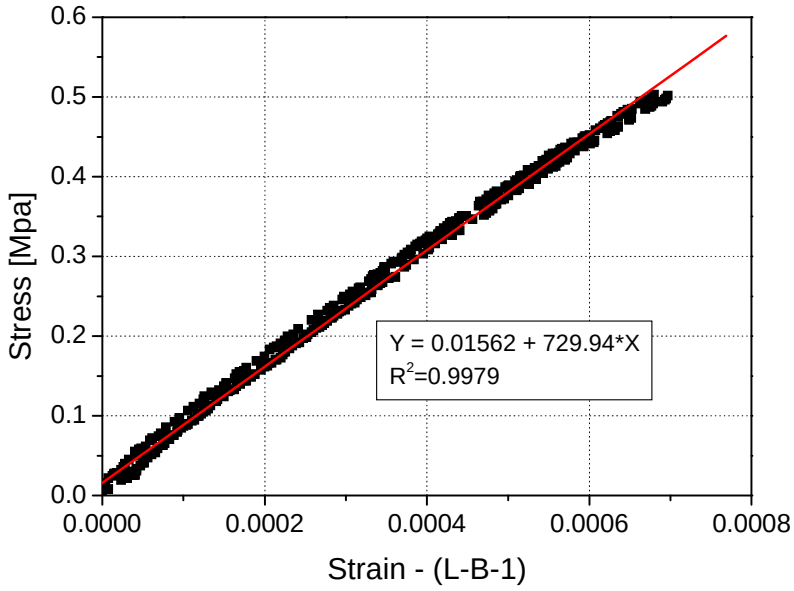

Figure 7: The relationship between the measured longitudinal strain at the bottom of section 1 (L-B-1) and corresponding calculated stress

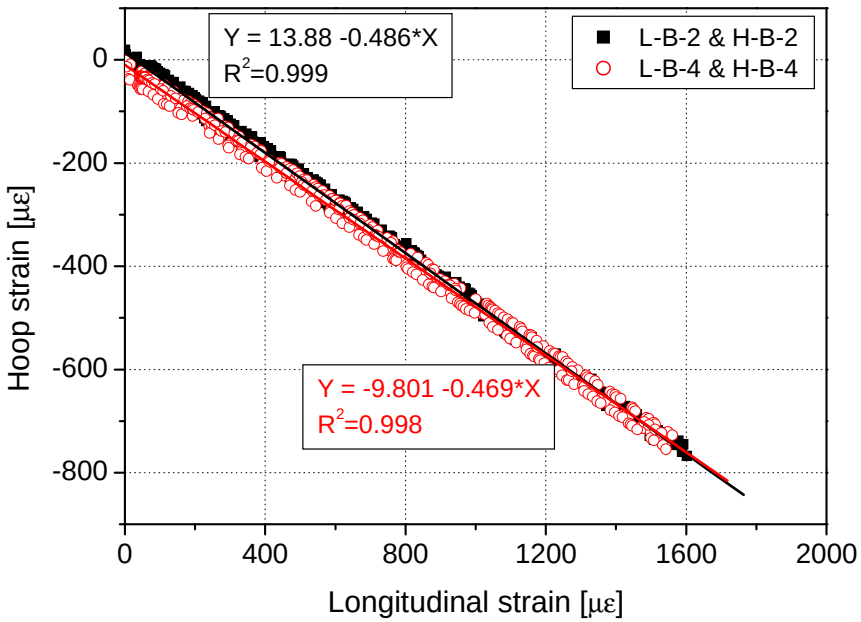

Figure 8: The relationships between hoop and longitudinal strains measured at the bottom of section 2 and 4.

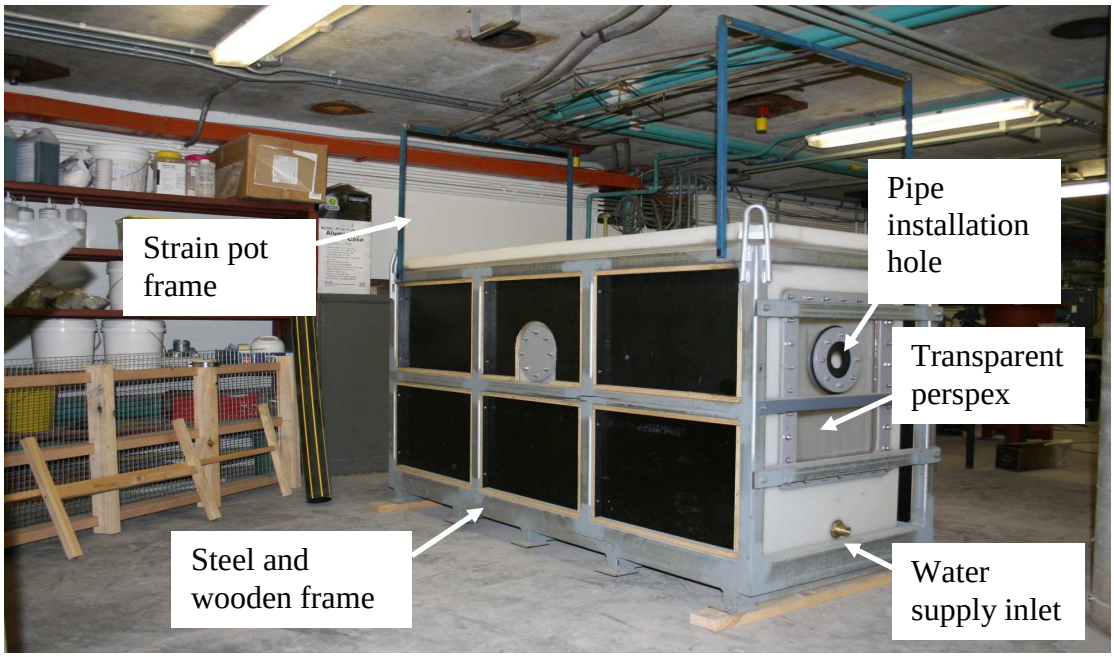

Figure 9: The box used for the experiment

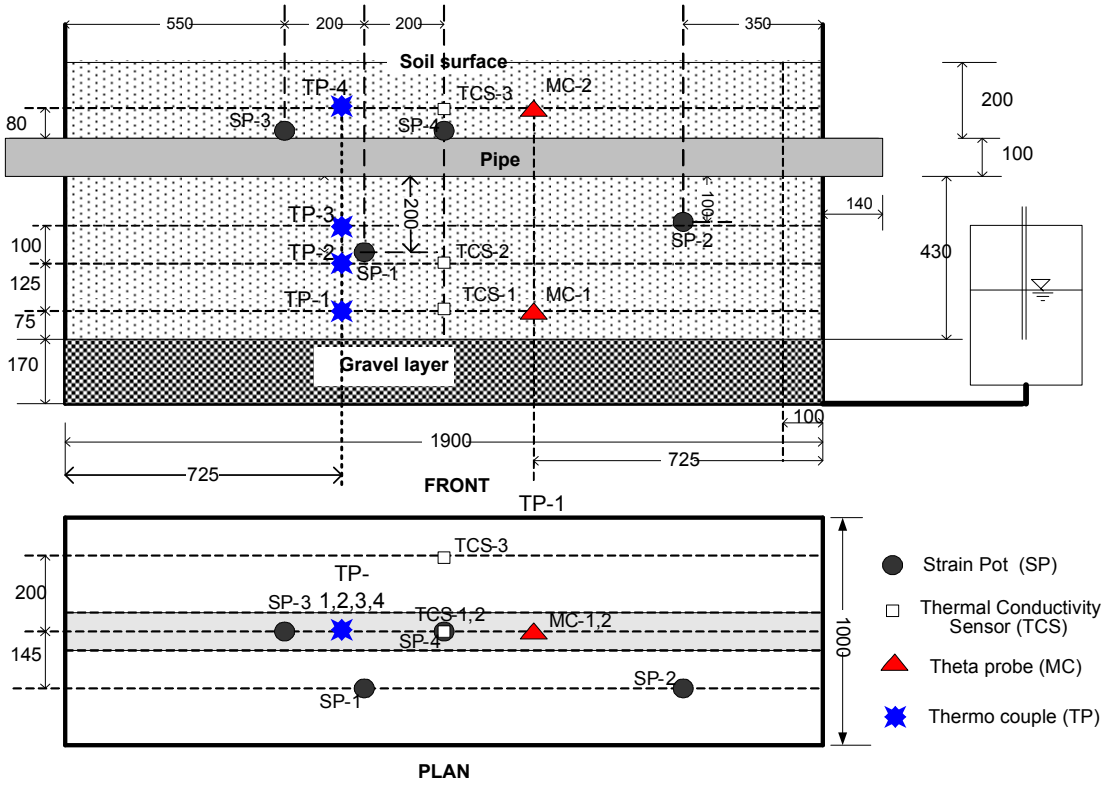

Figure 10: The schematic diagram of the soil box with sensor positions

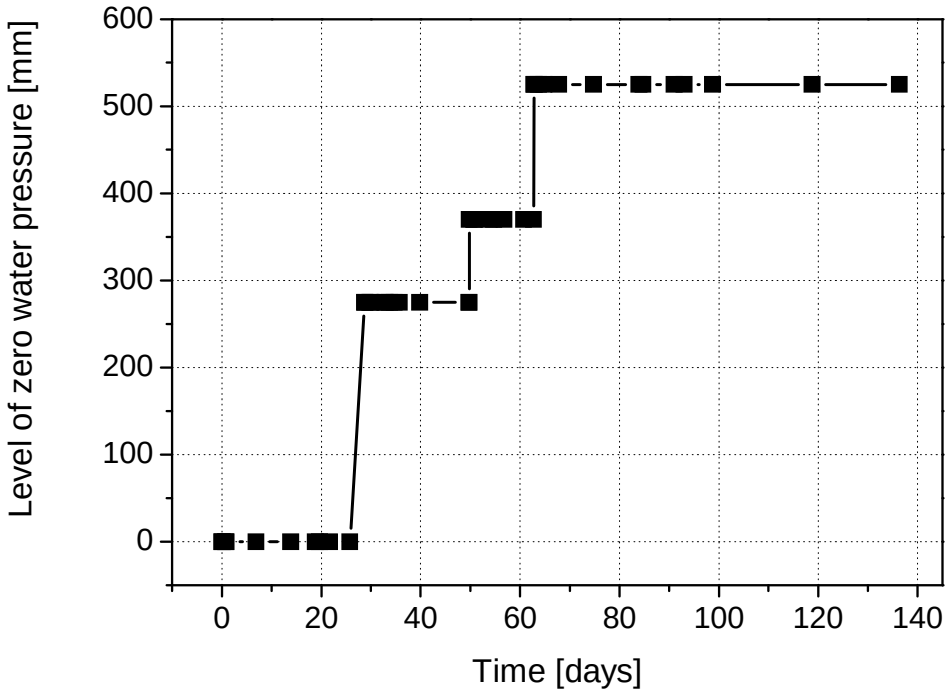

Figure 11: Rise of the level of zero water pressure against time

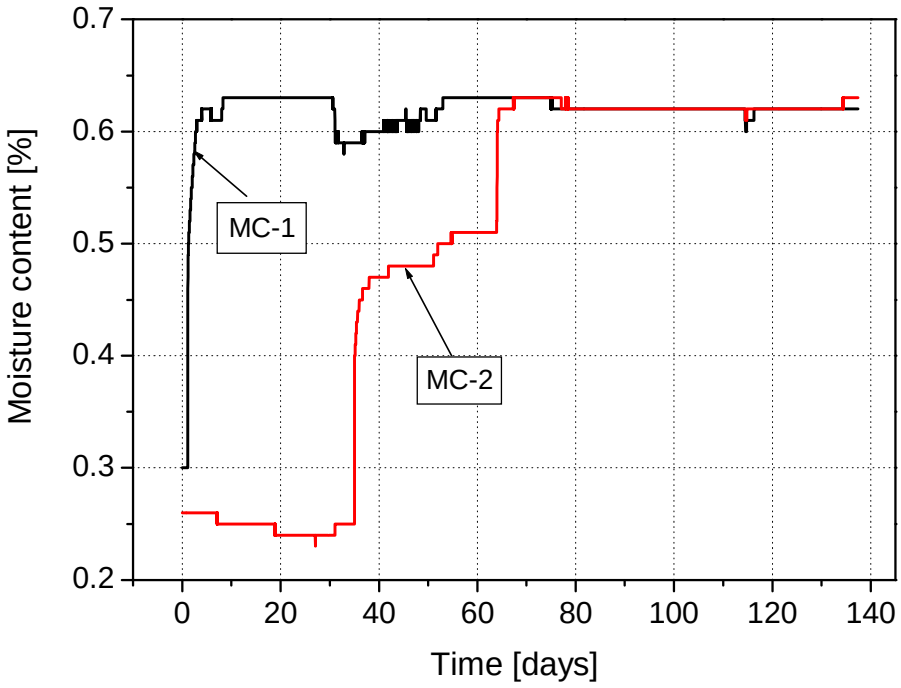

Figure 12: Change of volumetric water content against time

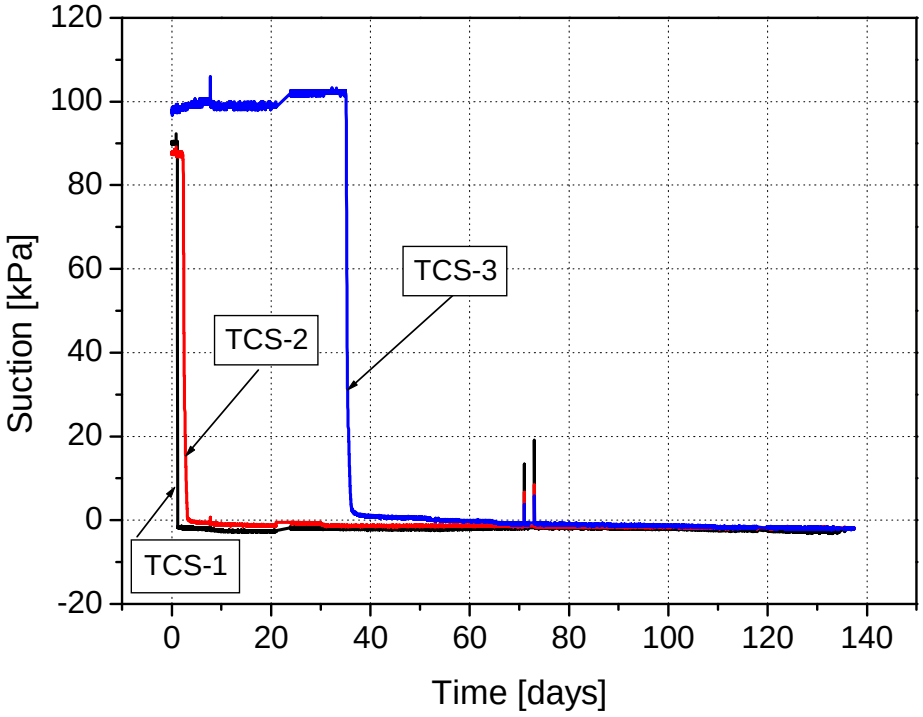

Figure 13: Soil suction change against time

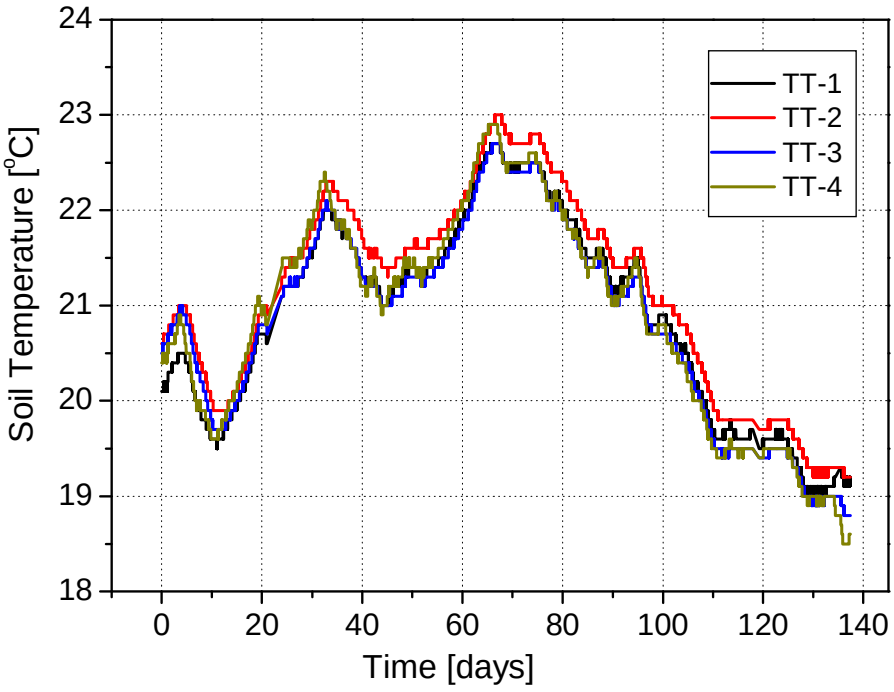

Figure 14: Time history of soil temperature change at different levels

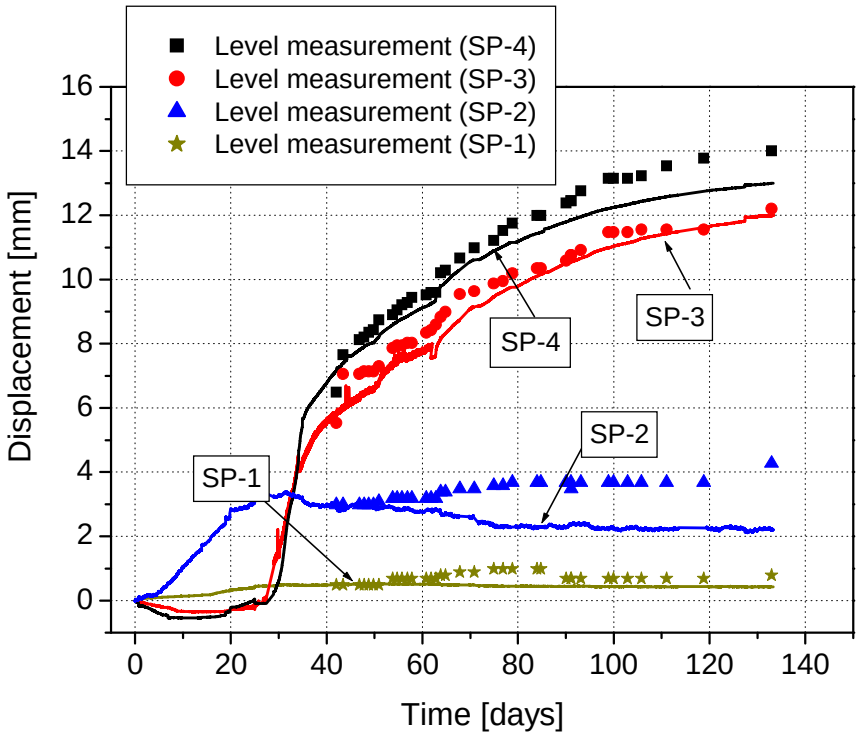

Figure 15: Time history of measured soil displacement at different levels (Solid lines show the continuous strain pot measurements, whereas the symbols show intermittent measurements taken by a survey level)

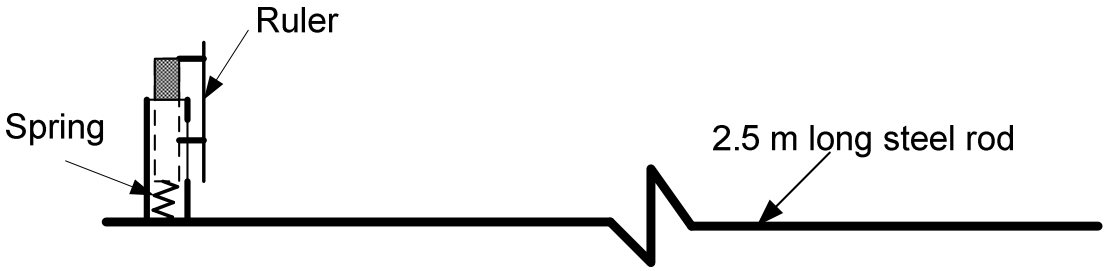

Figure 16: The device used in the pipe to measure its deflection

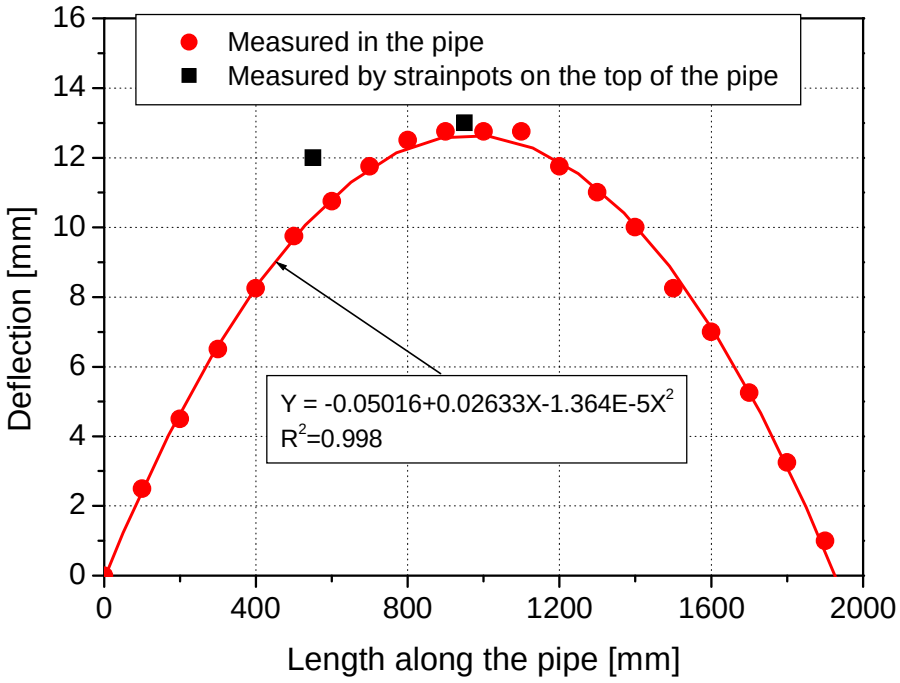

Figure 17: Comparison of pipe deflection measured internally using the specially designed device and strainpots located on the pipe

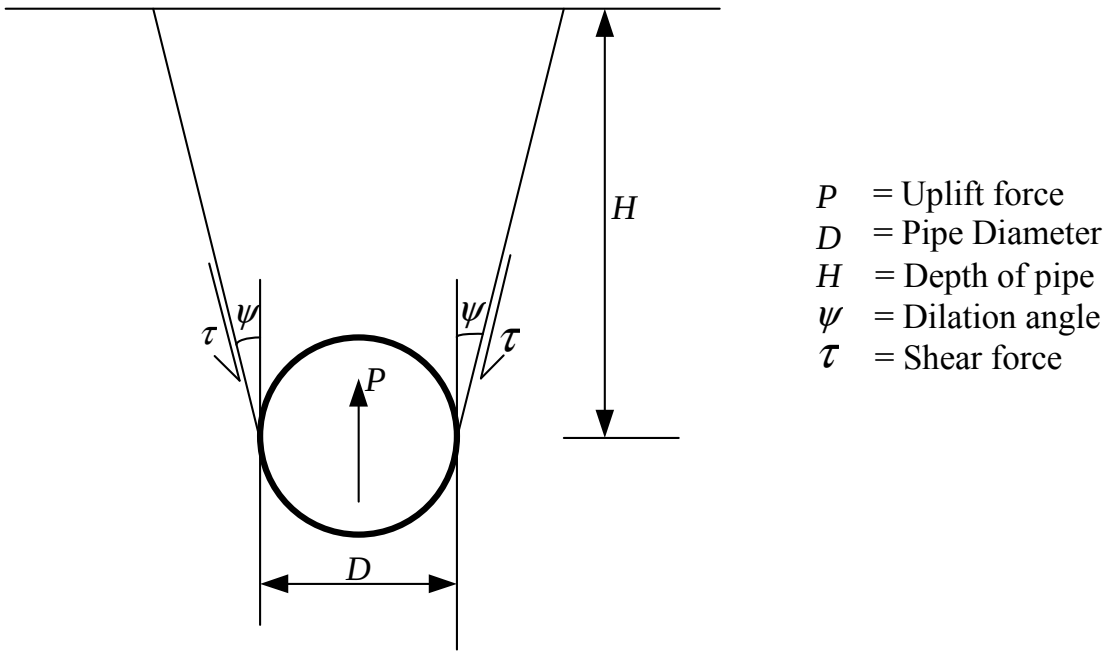

Figure 18: A model for predicting the peak uplift resistance (Cheuk et al. 2005)

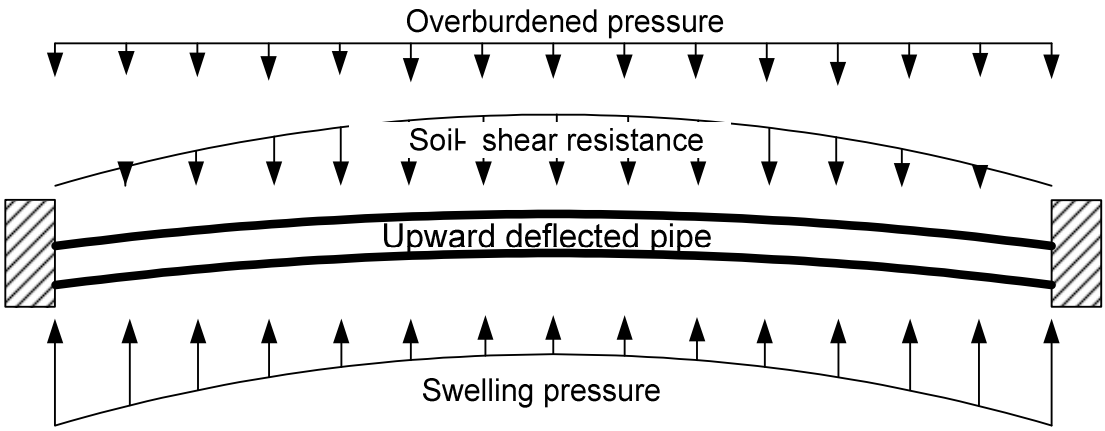

Figure 19: External stresses acting on a deflected buried pipe

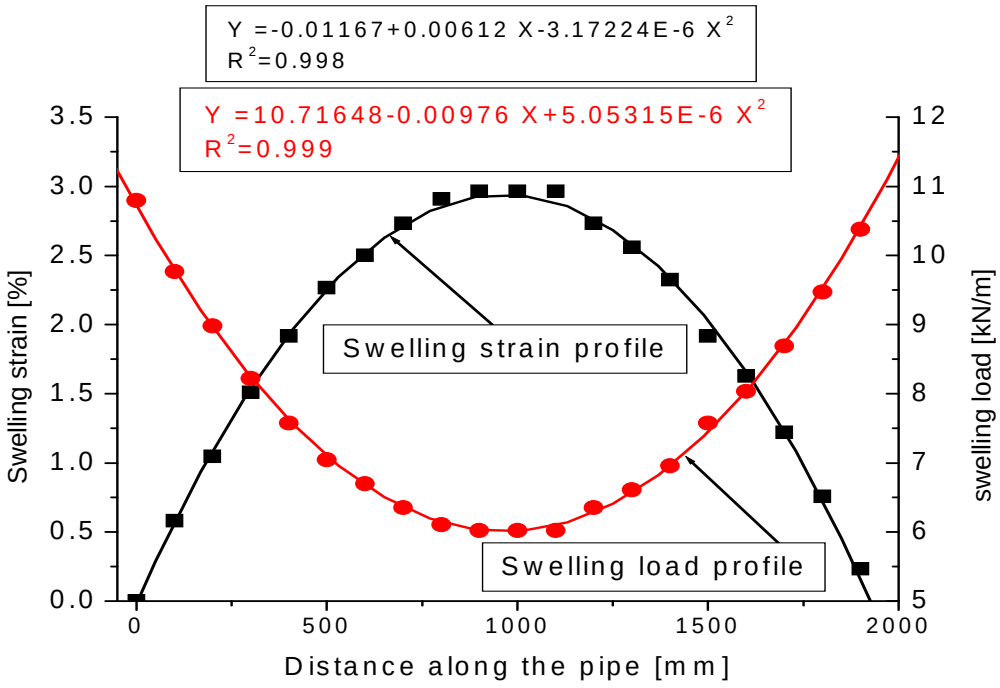

Figure 20: Swelling strain and swelling load used for the numerical analysis

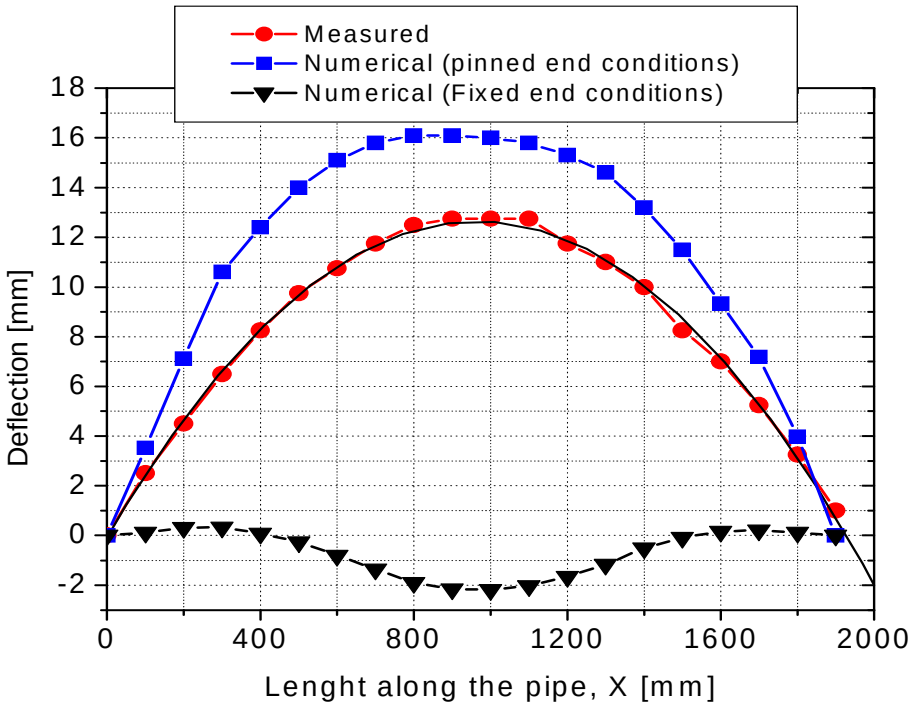

Figure 21: Comparison of analytical and experimental pipe deflections

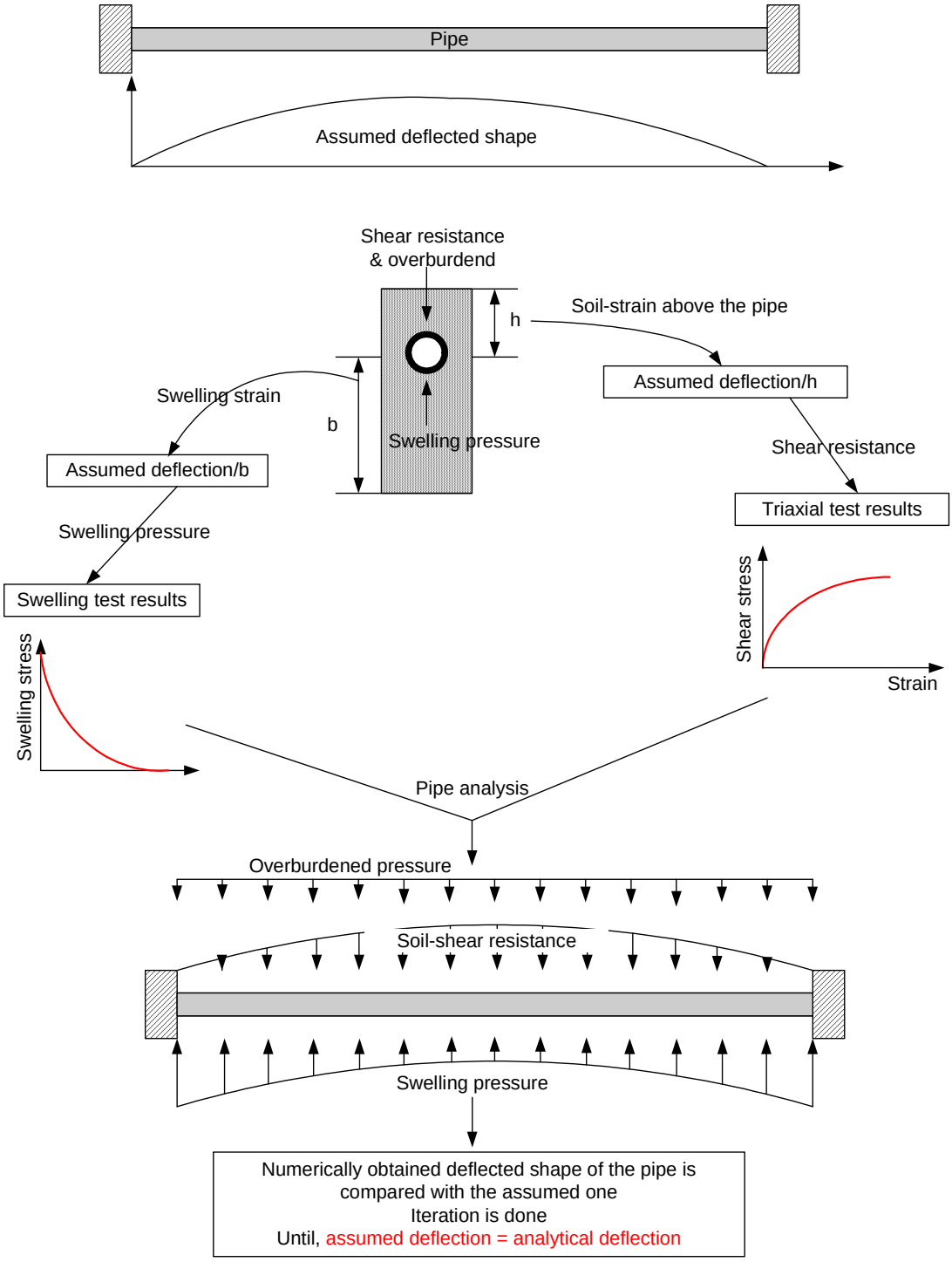

Figure 22: The schematic diagram of the proposed iterative analytical procedure to predict buried pipe deflection due to soil swelling